

Study the fading mechanism of LiMn_2O_4 battery with spherical and flake type graphite as anode materials

Hung-Chun Wu^a, Zheng-Zhao Guo^a, Hsiang-Ping Wen^b, Mo-Hua Yang^{a,*}

^a Material Research Laboratories, Industrial Technology Research Institute, Taiwan

^b Instrumentation Center, National Taiwan University, Taiwan

Available online 31 May 2005

Abstract

The fading mechanism of Li ion batteries with two different anode materials was discussed in this study. Anode materials were spherical type of meso-phase carbon micro bead (MCMB) and flake type of pitch coated graphite (PCG). This battery used LiMn_2O_4 as the cathode materials. The LiMn_2O_4 /MCMB battery had higher rate capability than the LiMn_2O_4 /PCG battery. However, the LiMn_2O_4 /PCG battery had only 20% capacity retention after 70 cycling tests, while the LiMn_2O_4 /MCMB battery had 95% capacity retention. The X-ray diffraction (XRD) and X-ray photospectroscopy (XPS) were used to analyze the structure of active materials and the solid electrolyte interface (SEI) films on the electrodes. It was found that structure of PCG anode and LiMn_2O_4 cathode was maintained as pristine structure by XRD analysis. The carbonate was easier to decompose on PCG surface than on the MCMB surface by XPS analysis. It was suggested that the electrolyte decomposition on PCG surface might be play a major role for the LiMn_2O_4 /PCG battery fading.

© 2005 Elsevier B.V. All rights reserved.

Keywords: Fading mechanism; Li ion batteries; LiMn_2O_4 ; MCMB; PCG

1. Introduction

Lithium ion secondary batteries have long been an attractive power source for a wide variety of applications. Spinel- LiMn_2O_4 and its derivatives are considered as promising materials for the positive electrodes of lithium rechargeable batteries. This is due to its good thermal stability, low cost and environmental friendliness. In large-scale high power battery, the LiMn_2O_4 was used as the cathode and meso-phase carbon micro bead (MCMB) was used as the anode [1–4]. However, the disadvantages of MCMB were high cost and low specific capacity. Flake type of artificial graphite could be the alternative material for anode due to its high specific capacity and low cost.

In this study, the performance and fading mechanism of lithium ion batteries are studied by using LiMn_2O_4 as the cathode material. Two different types of graphite were studied as the anode materials, namely spherical type of

MCMB and flake type graphite of pitch coated graphite (PCG).

2. Experimental

2.1. Battery preparation

The 18650 type Li ion batteries were consisted of LiMn_2O_4 as the cathode. Anode materials were either PCG (from Osaka gas) or MCMB (from Osaka gas) as the anode. The electrolyte was 1 M LiPF_6 in a mixture of ethylene carbonate (EC)/methyl-ethylene carbonate (MEC) 1:2 by volume (from Samsung). The properties of MCMB and PCG are shown in Table 1.

2.2. Electrochemical measurements

The rate capability test of the batteries were firstly charged at 0.2 C rate to 4.2 V and then discharged at 0.2, 1, 2 and 3 C rates, respectively. All tests were carried out with cut-off

* Corresponding author. Tel.: +886 3 5915234; fax: +886 3 5820039.
E-mail address: mhyang@itri.org.tw (M.-H. Yang).

Table 1
The properties of MCMB and PCG

	MCMB	PCG
Particle size (μm)	~ 10	~ 17
Shape	Spherical	Flake
First reversible capacity (mAh g^{-1})	300	355

voltages of 2.8 V and at ambient temperature. For the cycling test, currents for charge–discharge were held at 1 C rate.

2.3. Surface and structure analysis

Batteries for the X-ray photoelectron spectroscopy (XPS) analysis were (1) before cycling and (2) after 70 cycles discharged to 2.8 V. Then, the batteries were disassembled. The cathode and anode were extracted and washed in di-ethyl carbonate (DEC) solution and then dried under vacuum to remove the salt and solvent in the electrodes [5].

XPS measurement was taken on the ESCALAB 250 system (VG Scientific) by using monochromatized Al $K\alpha$ ray as the X-ray source ($h\nu = 1486.6 \text{ eV}$). The pass energy was 10 eV and the energy step was 0.05 eV. The pressure in the chamber is controlled below 6×10^{-9} Torr. The sample etching for depth profile was carried out with Ar ion sputtering. The depth profile was obtained at a sputtering rate of 1 nm min^{-1} on a SiO_2 sample.

The X-ray diffraction (XRD, MAC Science, MXP18) of Cu $K\alpha$ radiation was used to characterize the structure of anode and cathode. The content of Mn species in the anode was analyzed by ICP-AES (Jarrell-Ash, ICAP 9000).

3. Results and discussion

The test results of battery capacity at different discharge rates are shown in Fig. 1. The discharge capacity of $\text{LiMn}_2\text{O}_4/\text{MCMB}$ and $\text{LiMn}_2\text{O}_4/\text{PCG}$ batteries were 0.56 Ah at 0.2 C discharge current, while the capacity of $\text{LiMn}_2\text{O}_4/\text{MCMB}$ and $\text{LiMn}_2\text{O}_4/\text{PCG}$ were 0.53 and

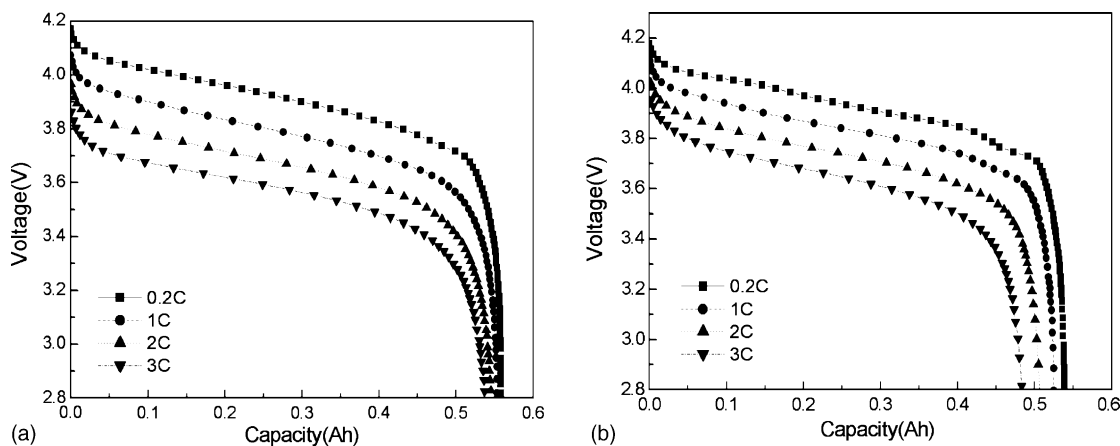


Fig. 1. The battery capacity of: (a) $\text{LiMn}_2\text{O}_4/\text{MCMB}$ and (b) $\text{LiMn}_2\text{O}_4/\text{PCG}$ batteries at different discharge rate.

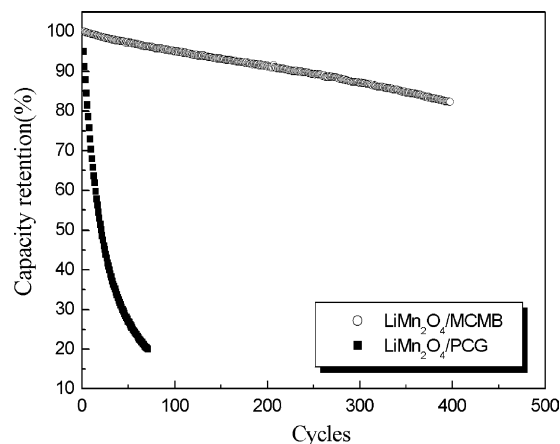


Fig. 2. The cycling test of $\text{LiMn}_2\text{O}_4/\text{MCMB}$ and $\text{LiMn}_2\text{O}_4/\text{PCG}$ batteries.

0.48 Ah at 3 C discharge rate. Although the discharge characteristics between $\text{LiMn}_2\text{O}_4/\text{MCMB}$ and $\text{LiMn}_2\text{O}_4/\text{PCG}$ batteries were close to each other, the rate capacity of $\text{LiMn}_2\text{O}_4/\text{MCMB}$ battery is higher than that of $\text{LiMn}_2\text{O}_4/\text{PCG}$ battery at 3 C discharge rate. Nevertheless, in Fig. 2, the cycling test result shows a significant difference between the $\text{LiMn}_2\text{O}_4/\text{MCMB}$ and $\text{LiMn}_2\text{O}_4/\text{PCG}$ battery. After 70 cycling tests, a $\text{LiMn}_2\text{O}_4/\text{PCG}$ battery had tremendous capacity loss and remained only 20% capacity retention, while $\text{LiMn}_2\text{O}_4/\text{MCMB}$ battery still had 95% capacity retention. After 400 times cycling test, the $\text{LiMn}_2\text{O}_4/\text{MCMB}$ battery had 80% capacity retention.

It has been reported that the fading mechanism in spinel-Mn Li ion batteries was due to the Mn dissolution from spinel-Mn cathode and then it was deposited on anode surface [6,7]. In addition, the Mn dissolution could also result in the structure instability of the cathode. To investigate the Mn effect on the anode surface, the Mn content of the anode after the cycling test was analyzed by ICP analysis. The results show that 365 ppm of Mn was deposited on the MCMB surface in the $\text{LiMn}_2\text{O}_4/\text{MCMB}$ battery after 300 cycling tests. For the $\text{LiMn}_2\text{O}_4/\text{PCG}$ battery, 178 ppm of Mn was deposited on the

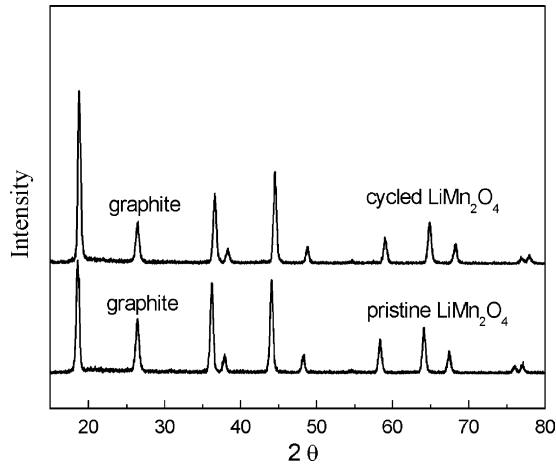


Fig. 3. The XRD patterns of a pristine LiMn_2O_4 and a cycled LiMn_2O_4 cathode from $\text{LiMn}_2\text{O}_4/\text{PCG}$ battery.

PCG surface after 70 cycling test. In this study, we found that after the long cycling test of $\text{LiMn}_2\text{O}_4/\text{MCMB}$ battery, large amount of Mn deposition on MCMB surface does not lead to the significant capacity fading of $\text{LiMn}_2\text{O}_4/\text{MCMB}$ battery. The $\text{LiMn}_2\text{O}_4/\text{MCMB}$ battery had 80% capacity retention, even after 400 times cycling test. Thus, other fading mechanism should be responsible to the battery fading.

Fig. 3 compared the XRD patterns of LiMn_2O_4 obtained from the pristine to the one obtained from the cycled cathode electrodes of $\text{LiMn}_2\text{O}_4/\text{PCG}$ battery. The LiMn_2O_4 retained its structure after cycling test. These results indicated that battery fading was not caused by the cathode structure degradation of the $\text{LiMn}_2\text{O}_4/\text{PCG}$ battery. The XRD patterns of the pristine and the cycled PCG electrodes in the $\text{LiMn}_2\text{O}_4/\text{PCG}$ battery were shown in Fig. 4. There was no obvious difference on the main (002) peak at $2\theta = 26.5^\circ$ between the pristine and the cycled PCG anode. Nevertheless, the second peak at $2\theta = 54.6^\circ$ had lower intensity of the cycled PCG electrode as compared to the intensity of pristine PCG graphite. Two possible factors had been proposed and discussed from Aurbach's work [8]. One was that the

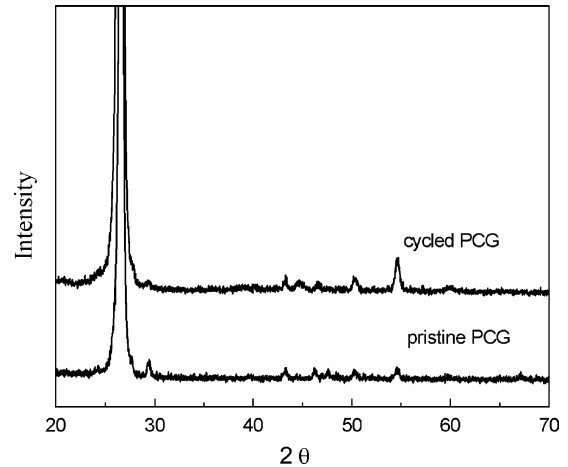


Fig. 4. The XRD patterns of a pristine PCG and a cycled PCG anode.

film formation on PCG surface might lead to the intensity diminution of XRD pattern due to the mask effect after cycling test. The other was the orientation change of particle due to gas evolution during film formation. Both hypotheses indicate that the solid electrolyte interface (SEI) film could play an important role for the fading of $\text{LiMn}_2\text{O}_4/\text{PCG}$ battery.

The C1s and O1s XPS spectra of the SEI film on the MCMB and PCG electrodes before cycling were shown in Figs. 5 and 6, respectively. The C1s peak near 284.3 eV was expected to be polyolefines and the broad peak around 285.5 eV was assigned to C–O–H and/or C–O–C bonds from solvent decomposition. The deposition of $\text{R-CH}_2\text{OCOOLi}$ or $(\text{CH}_2\text{OCO}_2\text{Li})_2$ corresponded to peaks at 286–287 eV. In Figs. 5a and 6a, the peak at 290 eV on the surface of MCMB and PCG anodes that might be related to the carbonate or semi-carbonate deposition and the shoulder appearing in the vicinity of 291 eV could responded to lithium carbonate [9–11]. For the O1s analysis, the broad peak around 532.5 eV was C–O bonding in the carbonyl structure and the peak of lithium carbonate was appeared in the vicinity of 534 eV. In

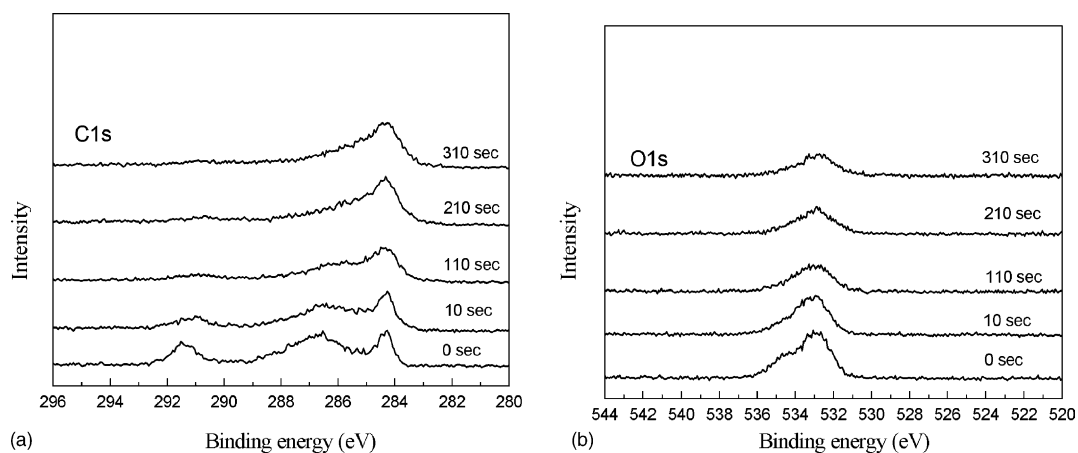


Fig. 5. XPS analysis of MCMB electrode before battery cycling test: (a) C1s and (b) O1s.

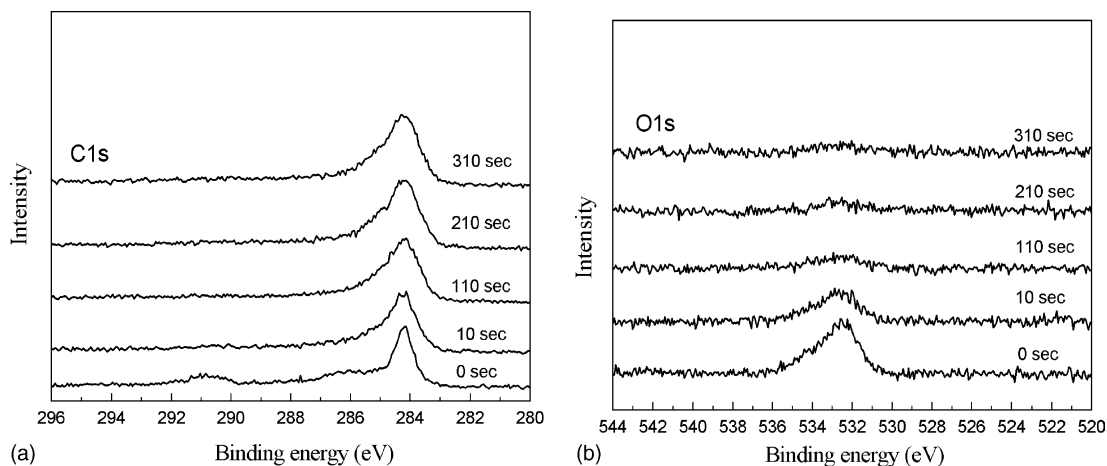


Fig. 6. XPS analysis of PCG electrode before battery cycling test: (a) C1s and (b) O1s.

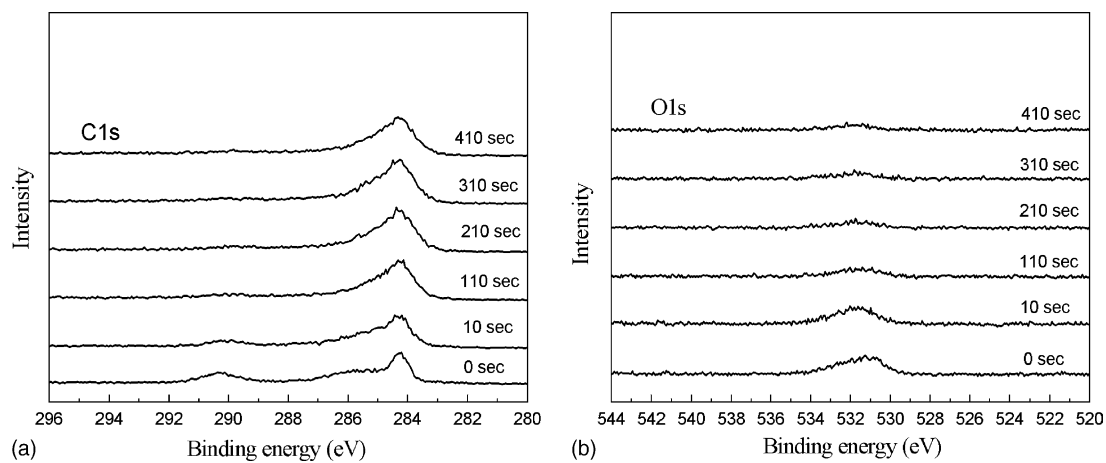


Fig. 7. XPS analysis of MCMB electrode after battery cycling test: (a) C1s and (b) O1s.

Fig. 6b, the intensity of O1s peak in PCG decrease with increasing sputtering time. But the O1s peaks in MCMB electrode could be found even after 310 s sputtering (Fig. 5b). It might be because of that SEI on the PCG surface was thinner

than that on the MCMB surface before the cycling test of battery.

The XPS spectra of cycled PCG and MCMB electrodes were shown in Figs. 7 and 8. In Fig. 7a and b, the C1s and

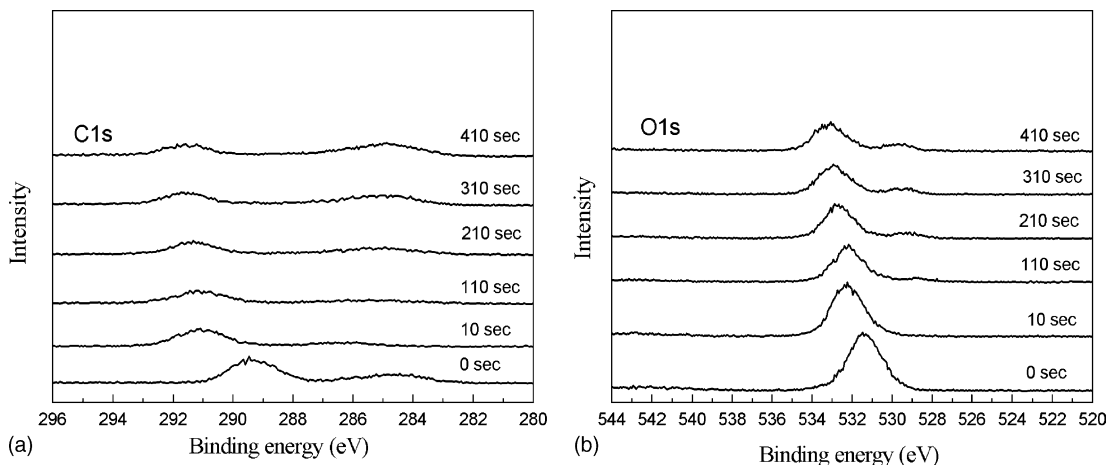


Fig. 8. XPS analysis of PCG electrode after battery cycling test: (a) C1s and (b) O1s.

O1s peak intensity of MCMB electrode surface was slight decreased with increasing sputtering time. Carbonate peak around 290 eV in C1s spectra was disappeared after sputtering. There were no significant changes on the MCMB surface structure after battery cycling test. This implied that a SEI forming on the surface of MCMB electrode before the battery cycling test. The SEI suppressed the electrolyte decomposition by making a thin stable interphase between electrolyte and anode during cycling test. On the other hand, the result shown that the composition of PCG surface was altered after battery cycling test. In Fig. 8a, an obvious carbonate signals (at around 290 eV) still could be found on the PCG C1s after 410 s sputtering. But this carbonate peak was not found in the bulk SEI structure on the PCG electrode before the cycling test (Fig. 6a). The carbonate deposition might be induced from the continuously electrolyte decomposition during the $\text{LiMn}_2\text{O}_4/\text{PCG}$ battery cycling test. In Fig. 8b, the similar observation could be detected in the O1s spectra on the cycled PCG surface of $\text{LiMn}_2\text{O}_4/\text{PCG}$ battery. Around 532.5–534 eV, carbonyl and lithium carbonate peaks were observed even after 410 s sputtering. These data further support our hypothesis that the electrolyte decomposition was take place on the PCG surface after battery cycling test. The thickness of SEI film became thicker on the PCG surface due to the electrolyte decomposition after the cycling test. This could be the major factor lead to the dramatic capacity fading in the cycling test of $\text{LiMn}_2\text{O}_4/\text{PCG}$ battery. Similar observation had also been mentioned from Yanagida's work [12].

4. Conclusion

From our battery test result, the $\text{LiMn}_2\text{O}_4/\text{MCMB}$ battery had a good rate capability and cycling performance than that of $\text{LiMn}_2\text{O}_4/\text{PCG}$ battery. Structure characterization and surface composition analysis were conducted to find the battery

fading mechanism in $\text{LiMn}_2\text{O}_4/\text{PCG}$ battery. The structure of LiMn_2O_4 and PCG had no obvious change after cycling in the $\text{LiMn}_2\text{O}_4/\text{PCG}$ battery. In this study, we found that the PCG had thicker SEI film than that on the MCMB surface after cycling test. A significant decomposition of electrolyte was proposed to form the SEI film on the PCG surface after cycling test. It suggested that the electrolyte decomposition on the PCG surface play a major role for the performance fading of $\text{LiMn}_2\text{O}_4/\text{PCG}$ battery. A stable SEI formation mechanism was important when the PCG was considered as a candidate for the anode material in the LiMn_2O_4 battery system.

References

- [1] M.H. Yang, J.C. Fang, S.F. Yeh, The 20th International Electric Vehicle Symposium and Exposition, USA, November, 2003.
- [2] S. Kim, LG Chem Ltd., The 20th International Electric Vehicle Symposium and Exposition, USA, November, 2003.
- [3] M.H. Yang, J.C. Fang, H. Wu, C.T. Yao, The Proceeding of the 20th International Electric Vehicles Symposium, Busan, Korea, October, 2002.
- [4] M.H. Yang, J.C. Fang, S.F. Yeh, J.H. Tsai, H.C. Wu, Fifth Advanced Batteries and Accumulators International Conference, Czech Republic, 2004.
- [5] T. Eriksson, T. Gustafsson, J.O. Thomas, *Electrochem. Solid State Lett.* 5 (2002) 35.
- [6] H. Tsunekawa, S. Tanimoto, R. Marubayashi, M. Fujita, K. Kifune, M. Sano, *J. Electrochem. Soc.* 149 (2002) 1326.
- [7] S. Komaba, N. Kumagai, Y. Kataoka, *Electrochim. Acta* 47 (2002) 1229.
- [8] D. Aurbach, B. Markovsky, A. Rodkin, M. Cojocaru, E. Levi, H. Kim, *J. Electrochim. Acta* 47 (2002) 1899.
- [9] V. Eshkenazi, E. Peled, L. Burstein, D. Golodnitsky, *Solid State Ionics* 170 (2004) 83.
- [10] A.M. Andersson, K. Edstrom, *J. Electrochem. Soc.* 148 (2001) 1100.
- [11] D. Bar-Tow, E. Peled, L. Burstein, *J. Electrochem. Soc.* 146 (1999) 824.
- [12] K. Yanagida, A. Yanai, Y. Kida, A. Funahashi, T. Nohma, I. Yonezu, *J. Electrochem. Soc.* 149 (2002) 804.